(3) E. O. Fischer and K. Öfele, *Chem. Ber.*, **91**, 2395 (1958).
(4) (a) F. Mathey, *J. Organomet. Chem.*, **93**, 377 (1975); (b) *Tetrahedron Lett.*, **46**, 4155 (1976).
(5) B. Chevrier and R. Weiss, *J. Am. Chem. Soc.*, **97**, 1416 (1975).
(6) P. A. Doyle and P. S. Turner, *Acta Crystallogr., Sect. A*, **24**, 390 (1968).
(7) R. F. Stewart, E. R. Davidson, and W. T. Simpson, *J. Chem. Phys.*, **42**, 3175 (1965).
(8) D. T. Cromer and D. Liberman, *J. Chem. Phys.*, **53**, 1891 (1970).
(9) G. Germain, P. Main, and M. M. Woolfson, *Acta Crystallogr., Sect. B*, **26**, 274 (1970).
(10) Supplementary material.
(11) L. F. Dahl and R. E. Rundle, *Acta Crystallogr.*, **16**, 419 (1963).
(12) R. Bau, S. W. Kirtley, T. N. Sorrell, and S. Winarko, *J. Am. Chem. Soc.*, **96**, 988 (1974).
(13) E. H. Schubert and R. K. Sheline, *Z. Naturforsch. B*, **20**, 1306 (1965).
(14) P. Coggon and A. T. McPhail, *J. Chem. Soc., Dalton Trans.*, 1888 (1973).
(15) J. A. Jarvis, R. H. B. Mais, and P. G. Owston, *J. Chem. Soc. A*, 1473 (1968).
(16) L. D. Quin, J. G. Bryson, and C. G. Moreland, *J. Am. Chem. Soc.*, **91**, 3308 (1969).

Contribution from the Molecular Structure Corporation, College Station, Texas 77840, and Department of Chemistry, Texas A&M University, College Station, Texas 77843

On the Mechanism of Ion Exchange in Zirconium Phosphates. 20. Refinement of the Crystal Structure of α-Zirconium Phosphate

J. M. TROUP and A. CLEARFIELD*

Received June 23, 1977 AIC70452+

The preparation of high-quality zirconium phosphate, $Zr(HPO_4)_2 \cdot H_2O$, crystals permitted refinement of the previously determined structure to the state where positional parameters of the exchangeable hydrogen atoms could be determined. A new unit cell, in space group $P2_1/n$ rather than the standard $P2_1/c$, was chosen because of its smaller β angle. The new cell dimensions are $a = 9.060$ (2) Å, $b = 5.297$ (1) Å, $c = 15.414$ (3) Å, $\beta = 101.71$ (2)° and $Z = 4$. Intensity data were collected by the θ–2θ scan procedure using an automated four-circle diffractometer (Enraf-Nonius CAD-4). Refinement of the data (2005 independent reflections with $I \geq 3\sigma(I)$ of 3178 measured) by the full-matrix least-squares procedure with anisotropic temperature factors for all nonhydrogen atoms resulted in a final R value of 0.027. The average Zr–O bond distance is 2.064 (5) Å. Each P–OH group forms a hydrogen bond with the water molecule (O–O distances 2.807 (3) and 2.769 (3) Å). The water molecule in turn acts as donor in forming one hydrogen bond with a P–O–H oxygen. The other water hydrogen is not involved in hydrogen bonding. There are no hydrogen bonds between layers so that only van der Waals forces must hold the layers together.

Introduction

Zirconium bis(monohydrogen orthophosphate) monohydrate, $Zr(HPO_4)_2 \cdot H_2O$, hereafter referred to as α-ZrP, is a crystalline ion exchanger with many interesting properties.[1] This compound has a layered structure in which the metal atoms lie nearly in a plane and are bridged by phosphate groups.[2] Three oxygens of each phosphate are bonded to three different zirconium atoms arranged at the apices of a near equilateral triangle. The fourth points away from the layer and bonds to a hydrogen atom. Adjacent layers are staggered in a pseudo-hexagonal fashion so as to form six-sided cavities between the layers. A water molecule sits in the center of each cavity.

Exchange occurs by replacement of the orthophosphate hydrogen by cations which then occupy positions between the layers.[3] It is not known whether the hydrogen atoms are present as covalent P–O–H or as hydronium ion. Infrared data are not conclusive on this point.[1] Formulation of a mechanism for the exchange precess would be greatly aided by a knowledge of the type and disposition of the hydrogen atoms. This information was not forthcoming from the previous crystal structure determination. Crystals of α-ZrP tend to be disordered with streaked or broadened reflections the rule. Film methods were used to obtain intensity data and refinement could only be carried to partial completion ($R = 0.084$).[2] Errors (esd's) in the bond distances were 0.02–0.03 Å. Thus, many of the finer features of the structure, as well as the hydrogen atom positions and hydrogen bonding scheme, could not be ascertained with certainty. We have now been able to grow much better crystals which permitted a significant improvement in refinement of the structure. When this work was near completion, it came to our attention that a neutron diffraction study had been carried out on α-ZrP powders to determine the hydrogen atom positions.[4] The results of that study will be discussed along with our findings.

* To whom correspondence should be addressed at Texas A&M University.

Table I. Comparison of Present with Previously Determined Crystal Data

Unit cell constants	Present study	Previous study	
Space group	$P2_1/n$	$P2_1/c$	$P2_1/n$
a, A	9.060 (2)	9.076 (3)	
b, A	5.297 (1)	5.298 (6)	
c, A	15.414 (3)	16.22 (2)	15.41
β, deg	101.71 (2)	111.5 (1)	101.7
V, A^3	724.3 (5)	725.7	
d_{calcd}, g cm^{-3}	2.762	2.76	
d_{obsd}, g cm^{-3}		2.72	
Z	4	4	

Experimental Section

Crystals were grown by a variation of that described by Alberti and Torracca.[5] Zirconium phophate was dissolved in concentrated HF and the solution, contained in a 12-mm i.d. quartz tube, kept at 60–65 °C in an oil bath. In 17–48 h crystals formed on the walls of the tube. The contents were then poured into a boric acid solution. The fluoroborate precipitate which formed was separated from the zirconium phosphate crystals by extensive washing followed by decantation.

A pentagonal-shaped platelet 0.34 × 0.25 × 0.076 mm was mounted in a random orientation on a CAD-4 four-circle counter diffractometer (Enraf-Nonius). Accurate unit cell dimensions were determined from 25 reflections at high and moderate 2θ angles. A graphite crystal incident-beam monochrometer was used with Mo Kα radiation (λ(Mo Kα$_1$) 0.709 30 Å)). The data were collected at a takeoff angle of 5.6° using the θ–2θ scan technique. The results are collected in Table I

Table II. Positional and Thermal Parameters (Å²) and Their Estimated Standard Deviations[a]

Atom	x	y	z	B_{11}	B_{22}	B_{33}	B_{12}	B_{13}	B_{23}
Zr	0.24609 (2)	0.25261 (5)	0.48506 (2)	0.425	0.518	1.187	−0.004	0.171	−0.015
P2	0.38744 (7)	0.7508 (1)	0.38567 (4)	0.531	0.718	0.872	−0.008	0.160	−0.035
P3	−0.13422 (7)	0.2420 (1)	0.39658 (4)	0.494	0.634	0.887	−0.033	0.129	−0.028
O4	0.5445 (2)	0.8037 (4)	0.4374 (2)	0.622	1.515	2.099	0.002	−0.074	−0.335
O5	0.3353 (2)	0.4862 (4)	0.4007 (1)	1.604	0.611	1.930	−0.199	0.869	0.004
O6	0.2772 (2)	0.9480 (4)	0.4065 (1)	0.816	0.702	1.812	0.345	0.155	−0.295
O7	0.3885 (3)	0.7559 (5)	0.2843 (1)	2.084	2.317	1.037	−0.172	0.522	0.082
O8	−0.2180 (2)	0.4364 (4)	0.4404 (2)	1.230	0.907	2.148	0.173	0.661	−0.423
O9	−0.1554 (2)	−0.0205 (4)	0.4316 (1)	1.131	0.793	1.913	−0.213	0.529	0.313
O10	−0.1942 (2)	0.2493 (5)	0.2949 (1)	1.171	2.395	1.104	−0.636	−0.092	0.089
O11	0.0320 (2)	0.3070 (4)	0.4086 (2)	0.443	1.487	1.790	−0.179	0.054	0.501
O12	0.0042 (3)	0.7241 (5)	0.2617 (2)	1.954	2.017	3.213	−0.261	−0.080	0.236

Atom	x	y	z	B, Å²	Atom	x	y	z	B, Å²
H1	0.424 (5)	0.907 (9)	0.267 (3)	3.5 (11)	H3	0.043 (5)	0.815 (9)	0.247 (3)	2.9 (10)
H2	−0.261 (5)	0.245 (7)	0.280 (3)	2.4 (10)	H4	0.027 (4)	0.701 (7)	0.330 (3)	1.3 (8)

[a] The form of the anisotropic thermal parameter is $\exp[-1/4(B_{11}h^2a^{*2} + B_{22}k^2b^{*2} + B_{33}lc^{*2} + 2B_{12}hka^*b^* + 2B_{13}hla^*c^* + 2B_{23}klb^*c^*)]$.

where they are compared with the previously reported film data.[2] A new unit cell ($P2_1/n$) was chosen rather than the one with $P2_1/c$ symmetry[2] because of the smaller β angle. The appropriate transformation matrices for the cell dimensions and positional parameters are

$$\begin{bmatrix} A \\ B \\ C \end{bmatrix}_n = \begin{bmatrix} -1 & 0 & 0 \\ 0 & -1 & 0 \\ 1 & 0 & 1 \end{bmatrix} \begin{bmatrix} a \\ b \\ c \end{bmatrix}_c$$

and

$$\begin{bmatrix} X \\ Y \\ Z \end{bmatrix}_n = \begin{bmatrix} -1 & 0 & 1 \\ 0 & -1 & 0 \\ 0 & 0 & 1 \end{bmatrix} \begin{bmatrix} x \\ y \\ z \end{bmatrix}_c$$

where the capital letters refer to the n glide cell and lower case letters to the c glide cell. A comparison of the two cells is given in Table I.

Intensity data were collected on the same crystal under the following conditions. The crystal to counter distance was 21 mm and the crystal to aperture distance 17.3 cm. A θ–2θ scan method was used with a variable scan rate ranging from 20°/min for the most intense reflection to 2°/min for the weak ones. The angular scan width was variable and amounted to 0.6° before 2θ (Mo Kα) and 0.6° after 2θ (Mo Kα_2). Right and left backgrounds were each scanned for 25% for the total scan time. During data collection three standard reflections were recorded every 64 reflections and used to place the data on a common scale. The change in intensities of the standards was small and random, with maximum fluctuation about the mean of ±3%. A total of 3178 reflections were scanned out to $2\theta = 70°$. Of these 2005 had intensities with $I \geq 3\sigma(I)$ and were considered to be observed. Here $\sigma(I) = [S^2(C + R^2B) + (pI)^2]^{1/2}$ and $I = S(C - RB)$, where S = scan rate, C = total integrated peak count, R = ratio of scan time to background counting time, B = total background count, and $p = 0.05$. These data were corrected for Lorentz and polarization factors and also for absorption.[6] With $\mu = 19.54$ the transmission factors ranged from 0.692 to 0.870.

Refinement of the Structure

Refinement was carried out by the full-matrix least-squares method. The starting parameters including isotropic temperature factors were taken from the previous study.[2] Refinement proceeded smoothly to convergence, with anisotropic temperature factors, to an R_F value of 0.032. A difference Fourier, prepared from all the data, revealed two hydrogen atoms at reasonable bond distances but not the remaining two. Inspection of the data uncovered four reflections which had unsymmetrical background and whose $|F_o| - |F_c|$ values amounted to more than $3R_F$. These were rejected and refinement continued to $R_F = 0.029$ and $R_{wF} = 0.053$. A difference map was now prepared using only low-angle data (589 reflections below $(\sin\theta)/\lambda = 0.4$). Four hydrogen atoms were located at reasonable distances from O(7), O(10), and O(12). These were refined isotropically with all the data but two of the hydrogens moved to within 0.65 Å of their oxygens. Inspection of the data led to rejection of six more reflections. The two errant hydrogens were then placed at 0.95 Å from their bonded oxygens and again refined. Convergence was considered complete when all the shifts were less than one-tenth their standard deviations. The final reliability indices were $R_F = 0.027$ and $R_{wF} = 0.048$ and the esd of an observation of unit weight was 1.188. Here $R_F = (\sum||F_o| - |F_c||)/\sum|F_o|$, $R_{wF} = [\sum w(|F_o| - |F_c|)^2/\sum wF_o^2]^{1/2}$, $w = 1/\sigma^2(F_o)$, and $\sigma(F_o^2) = [\sigma(I)^2 + (0.05F^2)^2]^{1/2}/(Lp)$ where $F_o^2 = F^2/(Lp)$. The function minimized was $\sum w(|F_o| - |F_c|)^2$. Atomic scattering factors for all atoms were taken from the compilation of Cromer and Waber[7] and corrected for anomalous dispersion (both the real and imaginary parts).[8]

Final positional and thermal parameters are presented in Table II. A table of observed and calculated structure factors is available.[9] The final difference map was featureless with maxima and minima in the range ±0.3 e/Å³.

Table III. Bond Distances (Å)[a]

Zr–O4	2.048 (2)	P2–O4	1.510 (2)
Zr–O5	2.074 (2)	P2–O5	1.512 (2)
Zr–O6	2.071 (2)	P2–O6	1.524 (2)
Zr–O8	2.054 (2)	P2–O7	1.564 (2)
Zr–O9	2.065 (2)	P3–O8	1.517 (2)
Zr–O11	2.075 (2)	P3–O9	1.518 (2)
		P3–O10	1.551 (2)
		P3–O11	1.519 (2)

[a] Numbers in parentheses are estimated standard deviations in the least significant digits

Table IV. Bond Angles (deg)

O4–Zr–O5	91.14 (8)	O4–P2–O5	112.4 (1)
O4–Zr–O6	90.45 (7)	O4–P2–O6	110.5 (1)
O4–Zr–O8	89.76 (8)	O4–P2–O7	109.2 (1)
O4–Zr–O9	89.35 (8)	O5–P2–O6	111.4 (1)
O4–Zr–O11	178.85 (8)	O5–P2–O7	103.6 (1)
O5–Zr–O6	88.96 (7)	O6–P2–O7	109.6 (1)
O5–Zr–O8	88.88 (7)	O8–P3–O9	110.6 (1)
O5–Zr–O9	179.51 (7)	O8–P3–O10	109.2 (1)
O5–Zr–O11	89.96 (7)	O8–P3–O11	111.4 (1)
O6–Zr–O8	177.83 (8)	O9–P3–O10	109.8 (1)
O6–Zr–O9	91.04 (7)	O9–P3–O11	111.0 (1)
O6–Zr–O11	89.91 (7)	O10–P3–O11	104.7 (1)
O8–Zr–O9	91.12 (7)		
O8–Zr–O11	89.92 (8)		
O9–Zr–O11	89.55 (7)		
Zr–O4–P2	160.6 (1)	Zr–O8–P3	157.5 (1)
Zr–O5–P2	145.4 (1)	Zr–O9–P3	149.4 (1)
Zr–O6–P2	146.1 (1)	Zr–O11–P3	145.8 (1)

Results and Discussion

The refined structure as far as the nonhydrogen atoms are concerned is essentially the same as given previously.[2] However, the esd's are now about 0.1 of their former values. A list of bond distances is given in Table III and bond angles in Table IV. Certain features of the structure can now be discussed with certainty. The Zr–O octahedron is quite regular. The bond distances average 2.064 (5) Å.[10] All the

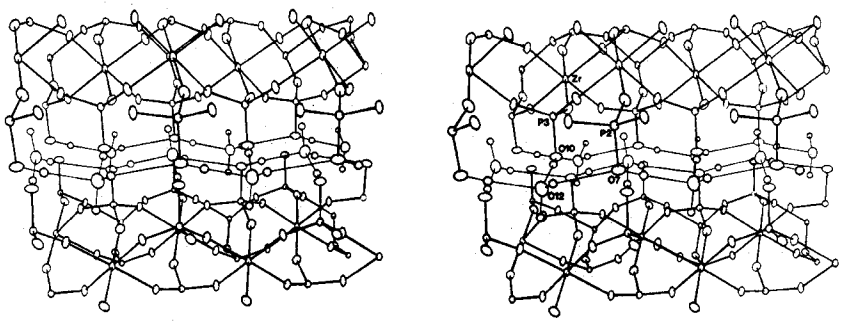

Figure 1. A stereoview of a portion of the structure of zirconium phosphate showing the arrangement of the layers and the hydrogen bonding scheme.

Table V. Hydrogen Bond Parameters

Donor	Hydrogen	Acceptor	D-H, Å	H···A, Å	D-H···A, deg
O7	H1	O12	0.92 (4)	1.89 (4)	176 (4)
O10	H2	O12	0.61 (4)	2.16 (4)	175 (6)
O12	H3	O7	0.67 (5)	2.49 (5)	157 (5)
O12	H4		1.04 (4)		

Angles, Deg

P2-O7-H1	112 (3)	H1-O12-H4	97 (2)
P3-O10-H2	120 (4)	H2-O12-H3	116 (4)
H1-O12-H2	111 (2)	H2-O12-H4	107 (2)
H1-O12-H3	109 (4)	H3-O12-H4	115 (5)

Distances, Å

O7-O12	2.807 (3)	O10-O12	2.769 (3)
O12-O7′	3.109 (3)		

O–Zr–O bond angles are very close to 90°. In the case of the phosphate groups, the oxygens not bonded to zirconium, i.e., P–OH, form P–O bonds that are significantly longer than the others. Also the O5–P2–O7 and O10–P3–O11 bond angles are significantly shorter than the expected tetrahedral angle but the average angle is 109.45°.

The most important new feature uncovered by the present study is the hydrogen bonding scheme. Two of the O–H distances are quite short and are undoubtedly in error. The average O–H distance found by neutron diffraction is 0.96 (3) Å.[4] The two bonding schemes agree in their main features. This is shown in stereo in Figure 1. Other views of the structure are given in ref 2. A water molecule resides in the center of each cavity and accepts two hydrogen bonds from the P–OH donor groups. Both of these P–OH groups P2–O7–H1 and P3–O10–H2 are in the same layer and form the short hydrogen bonds. The water molecule in turn acts as donor forming an O12–H3···O7′ bond also in the same layer. The other water hydrogen is not involved in hydrogen bond formation but points toward the top (or bottom) of the cavity. There are no hydrogen bonds between layers.

Recalculation of the size of the entranceways into the cavities reveals that the largest opening is now 2.61 Å instead of 2.64 Å. Other values are essentially unchanged.[3]

Alberti et al.[11] have recently shown that replacement of sodium ion by protons in $ZrNaH(PO_4)_2 \cdot 5H_2O$ yields different zirconium phophates dependent upon the nature of the α-ZrP used to prepare the sodium salt. Zirconium phosphate crystals obtained by slow precipitation from HF solution gave α-ZrP upon exchange of H^+ for Na^+. On the other hand crystals prepared by the refluxing procedure in H_3PO_4[12] produced varying amounts of θ-ZrP[1,3] as well as α-ZrP. Thus, it was suggested[11] that the two preparation methods yield two distinct phases of zirconium phosphate. The present study, which is based on the crystals prepared in HF, has shown that this is not the case since the structural results were similar to those obtained before.[2,4] Rather differences observed in ion-exchange behavior must result from the different degrees of crystal perfection. It has been shown that the unit cell dimensions and particularly the *c* axis increase with decreasing crystallinity.[13] Thus, it is reasonable to assume that the interlayer van der Waals forces also decrease in the same fashion and that the expanded layer phase, θ-ZrP, is favored by increased crystal imperfection.

Leigh and Dyer have proposed a structural model for α-ZrP in which half the exchangeable hydrogens are present as ions.[14] This would leave a large negative charge residing on the layers and result in a strong binding of the layers. Firmness of binding was offered as an explanation for the very low uptake of ions by α-ZrP (unless base was also added). This explanation cannot be correct as all of the exchangeable hydrogen is covalently bonded to phosphate oxygens. Rather we again suggest that the degree of crystallite perfection is the determining factor. The more perfect the layers the greater must the attraction between them be. Thus, zirconium phophates with a high degree of crystallinity must require appreciable energy to initiate and sustain exchange. Equilibration of such exchangers with aqueous metal ion salts results in exchange of only small (or micro) amounts of ions.[3,15] Thus, base must be added along with the salt to supply the needed energy through reaction with the exchangeable hydrogens.[4] However, we have found that as the crystallinity of the exchanger decreases, increasing amounts of ion may be exchanged without addition of base. This is in keeping with the idea that in the less crystalline exchangers the phosphate groups are shifted or tilted away from their normal positions.[13] Thus, the cavities would have a range of sizes rather than a relatively constant set of dimensions as in the fully crystalline exchanger. This would lead to a range of hydrogen bond energies and presumably to a weakening of the van der Waals forces as separate consequences of the disorder. Exchange could then occur up to a point where the larger cavities are filled. More explicit explanations must await a knowledge of the defect structure of zirconium phosphate. Such studies are in progress.

Acknowledgment. This work was supported by Grant No. CHE76-17237 from the National Science Foundation for which grateful acknowledgment is made.

Registry No. α-ZrP, 13933-56-7.

Supplementary Material Available: Listings of structure factors F_o and F_c (9 pages). Ordering information is given on any current masthead page.

References and Notes

(1) A. Clearfield, G. H. Nancollas, and R. H. Blessing in "Ion Exchange and Solvent Extraction", Vol. 5, J. A. Marinsky and Y. Marcus, Ed., Marcel Dekker, New York, N.Y., 1973, Chapter 1.
(2) A. Clearfield and G. D. Smith, *Inorg. Chem.*, **8**, 431 (1969).
(3) A. Clearfield, W. L. Duax, A. S. Medina, G. D. Smith, and J. R. Thomas, *J. Phys. Chem.*, **73**, 3424 (1969).
(4) J. Albertsson and Å. Oskarsson, *J. Phys. Chem.*, in press.
(5) G. Alberti and E. Torracca, *J. Inorg. Nucl. Chem.*, **30**, 317 (1968).
(6) All the programs used for this study were part of the Enraf-Nonius Structure Determination Package (SDP), Enraf-Nonius, Delft, Holland, 1975; revised 1977.

(7) D. T. Cromer and J. T. Waber, "International Tables for X-Ray Crystallography", Vol. IV, The Kynoch Press, Birmingham, England, 1974, Table 2.2B.
(8) D. T. Cromer, ref 7, Table 2.3.1.
(9) Supplementary material.
(10) Estimated standard deviations from the mean were calculated as $[\sum(\bar{X} - X)^2/(n(n-1))]^{1/2}$.
(11) G. Alberti, U. Constantino, and J. S. Gill, *J. Inorg. Nucl. Chem.*, **38**, 1733 (1976).
(12) A. Clearfield and J. A. Stynes, *J. Inorg. Nucl. Chem.*, **26**, 117 (1964).
(13) A. Clearfield, Å. Oskarsson, and L. Kullberg, *J. Phys. Chem.*, **78**, 1150 (1974).
(14) D. Leigh and A. Dyer, *J. Inorg. Nucl. Chem.*, **34**, 369 (1972).
(15) A. Clearfield, unpublished results.

Contribution from the Departments of Chemistry, University of Virginia, Charlottesville, Virginia 22901, and University of Illinois at Chicago Circle, Chicago, Illinois 60680

Structural and Magnetic Properties of $[M(C_5H_5NO)_6]L_2$ (M = Cu, Zn; L = ClO_4^-, BF_4^-)

C. J. O'CONNOR,[1a] E. SINN,*[1a] and R. L. CARLIN*[1b]

Received June 28, 1977 AIC704633

The perchlorate and fluoborate salts of the hexakis(pyridine *N*-oxide) complexes of copper(II) and zinc(II) have been studied at 25 °C by single-crystal x-ray diffraction and EPR and in the 1–20 K region by magnetic susceptibility and heat capacity measurements. The room temperature EPR shows site splitting consistent with a static Jahn–Teller distortion while the bulk susceptibilities are isotropic ($g = 2.3$) and exhibit a large Weiss constant ($\Theta = -2.3$ K). The magnetic heat capacity is analyzed in terms of the Heisenberg linear chain model. The complexes crystallize in the space group $R\bar{3}$ with the metal atom at the center of the unit cell, which imposes a center of inversion, and a threefold rotation axis at the metal atom. In the perchlorate complexes, the anions have one Cl–O bond along the threefold axis, pointing away from the anion. The BF_4^- anions in the other complexes are positionally disordered, the predominant position being the same as in the perchlorates while a minor position has a B–F bond pointing toward the anion along the threefold axis. The cations have near-octahedral coordination about the metal atom, with metal–ligand bond lengths of 2.102 and 2.087 Å for zinc and copper, respectively. Although the Jahn–Teller effect is dynamic in the crystal lattice, space group $R\bar{3}$, the distortions from trigonal symmetry are static on the EPR time scale up to ambient temperature, the first observation of this phenomenon. Crystal data: $[Cu(C_5H_5NO)_6](ClO_4)_2$, space group $R\bar{3}$, $Z = 1$, $a = 9.620$ (2) Å, $\alpha = 81.21$ (2)°, $R = 3.6\%$ for 1076 reflections; $[Cu(C_5H_5NO)_6](BF_4)_2$, space group $R\bar{3}$, $Z = 1$, $a = 9.621$ (2) Å, $\alpha = 81.46$ (2)°, $R = 3.8\%$ for 1221 reflections; $[Zn(C_5H_5NO)_6](ClO_4)_2$, space group $R\bar{3}$, $Z = 1$, $a = 9.632$ (2) Å, $\alpha = 81.07$ (2)°, $R = 3.8\%$ for 1234 reflections; $[Zn(C_5H_5NO)_6](BF_4)_2$, space group $R\bar{3}$, $Z = 1$, $a = 9.621$ (1) Å, $\alpha = 81.25$ (4)°, $R = 3.9\%$ for 1241 reflections.

Introduction

We report the crystal structure and magnetic properties of $[M(C_5H_5NO)_6]X_2$ (where M = Cu^{2+}, Zn^{2+}; X = ClO_4^-, BF_4^-).[2] Several other members of this series of hexakis(pyridine *N*-oxide)metal(II) salts have proved to be of interest,[3] since the discovery that the crystal of the perchlorate series possesses rhombohedral symmetry.[4,5] The crystal structure of $[Ni(C_5H_5NO)_6](BF_4)_2$ shows that the fluoborate compounds, although disordered with respect to the anion, are isomorphous with the perchlorate series.[6]

Magnetic studies on the perchlorate series have revealed a consistently strong axial distortion exerted on the ion by the ligand field of the pyridine *N*-oxides. The manganese,[4] cobalt,[7] and nickel[8,9] ions all exhibit large crystal field splittings. Moreover a variety of interesting magnetic ordering phenomena have been observed in these compounds.[10-12]

The study of this series of compounds is being extended to the $S = {}^1/_2$ copper(II) ion by means of magnetic susceptibility, heat capacity, and EPR measurements. Both the perchlorate and the fluoborate compounds are shown to have very similar magnetic trigonal distortions at room temperature, although they have strikingly different magnetic properties at lower temperatures. The BF_4^- complex behaves as an $S = {}^1/_2$ planar Heisenberg antiferromagnet[13] and the ClO_4^- behaves as an $S = {}^1/_2$ linear chain Heisenberg antiferromagnet.[12]

Experimental Section

Preparations. Following previous procedures,[14] $[Cu(C_5H_5NO)_6](ClO_4)_2$ and the diamagnetic zinc host compound were prepared by mixing together stoichiometric quantities of the hydrated metal perchlorates and purified pyridine *N*-oxide in methanol. The fluoborate analogue was prepared in a similar fashion. The metal fluoborate was prepared by the addition of fluoboric acid to the metal carbonate. Single crystals of $[Zn(C_5H_5NO)_6]X_2Cu^{2+}$ (X = ClO_4^-, BF_4^-) were prepared by mixing the hydrated zinc salt with 0.1–1.0% copper salt and causing them to react with the pyridine *N*-oxide. The crystals were grown by slow evaporation of concentrated DMF solutions in a dry atmosphere.

Magnetic and Heat Capacity Data. Magnetic susceptibilities and heat capacity were measured at zero field with equipment described previously.[15] The EPR spectra were recorded on a Varian E-109 EPR spectrometer operating at X-band (9.506 GHz). The crystals were mounted in a series of orientations for rotation experiments. The axes of rotation include [100], [100] × [010], and [100] × [111]. Alignment along these axes is estimated to be within 3°.

Crystal densities were measured by flotation in chloroform/bromoform/carbon tetrachloride mixtures.

Crystal data for $[Cu(C_5H_5NO)_6](ClO_4)_2$: $CuCl_2O_{14}N_6C_{30}H_{30}$, mol wt 833, space group $R\bar{3}$, $a = 9.620$ (2) Å, $\alpha = 81.21$ (2)°, $V = 862$ Å^3, $\rho_{calcd} = 1.62$ g cm^{-3}, $\rho_{obsd} = 1.59$ g cm^{-3}, μ(Mo Kα) = 9.1 cm^{-1}; crystal dimensions (distances in mm of faces from centroid): (100) 0.115, ($\bar{1}$00) 0.115, (010) 0.085, (0$\bar{1}$0) 0.085, (001) 0.10, (00$\bar{1}$) 0.10; maximum and minimum transmission coefficients: 0.88, 0.85.

Crystal data for $[Cu(C_5H_5NO)_6]BF_4$: $CuF_8O_6N_4C_{30}B_2H_{30}$, mol wt 808, space group $R\bar{3}$, $a = 9.621$ (2) Å, $\alpha = 81.46$ (2)°, $V = 864$ Å^3, $\rho_{calcd} = 1.57$ g cm^{-3}, $\rho_{obsd} = 1.55$ g cm^{-3}, μ(Mo Kα) = 7.7 cm^{-1}; crystal dimensions (mm from centroid): (100) 0.21, ($\bar{1}$00) 0.21, (010) 0.26, (0$\bar{1}$0) 0.26, (001) 0.16, (00$\bar{1}$) 0.16; maximum and minimum transmission coefficients: 0.84, 0.81.

Crystal data for $[Zn(C_5H_5NO)_6](ClO_4)_2$: $ZnCl_2O_{14}N_6C_{30}H_{30}$, mol wt 835, space group $R\bar{3}$, $a = 9.633$ (2) Å, $\alpha = 81.07$ (2)°, $V = 864$ Å^3, $\rho_{calcd} = 1.61$ g cm^{-3}, $\rho_{obsd} = 1.57$ g cm^{-3}, μ(Mo Kα) = 9.7 cm^{-1}; crystal dimensions (mm from centroid): (100) 0.21, (100) 0.21, (010) 0.26, (010) 0.26, (001) 0.19, (001) 0.19; maximum and minimum transmission coefficients: 0.78, 0.73.

Crystal data for $[Zn(C_5H_5NO)_6](BF_4)_2$: $ZnF_8O_6N_6C_{30}B_2H_{30}$, mol wt 808, space group $R\bar{3}$, $a = 9.621$ (1) Å, $\alpha = 81.25$ (4)°, $V = 862$ Å^3, $\rho_{calcd} = 1.56$ g cm^{-3}, $\rho_{obsd} = 1.54$ g cm^{-3}, μ(Mo Kα) = 8.4 cm^{-1}; crystal dimensions (mm from centroid): (100) 0.23, (100) 0.23, (010)